3.4 Plasma Data Sets

3.4.1 Polar/CAMMICE/MICS

This section provides a brief discussion of how the Polar CAMMICE/MICS Plasma data set used in the Space Plasma Model (SPM) was generated. It includes brief descriptions of the instrument, efficiencies, instrument calibration, and data analysis. Detailed descriptions of each of these aspects will be provided elsewhere.

3.4.1.1 Spacecraft

The NASA Polar Mission was a Heliophysics science mission launched on 24 February 1996 into a highly elliptical (1.7 x 9.4 R_E), 83.7° inclination orbit with a period of about 18 hours. Over the course of the mission the line of apsides precessed in latitude, orienting the apogee over the north pole early in the mission, over the equator later in the mission and finally over the south pole near the end of the mission. Polar had a spin period of about 6 seconds.

3.4.1.2 Detector

The Charge and Mass Magnetospheric Ion Composition Experiment (CAMMICE) includes the Magnetospheric Ion Composition Sensor (MICS) instrument which we use in the development of SPM. The MICS sensor was originally flown on VIKING (1986-1987), CRRES (1990-1991), then part of Polar/CAMMICE (1996-2002). Its strength lies in the combination of using three independent measurement techniques to uniquely determine the energy, mass, and charge state of the detected particles. The energy per charge is measured in an electrostatic analyzer, the velocity in a time-of-flight system, and total energy in a solid state detector. Details of the instrument are given by *Wilken et al.* [1992] and *Fritz et al.* [2003], and of the data processing are given by *Koga et al.* [1996].

The CAMMICE/MICS instrument changed modes throughout the mission. For our purposes, the most useful mode is “Mode 2” or “Rate Scaler Table 2”, operational from 7 March 1997 through 17 March 2000, when the MICS failed the first time. In this mode, MICS measures the “zero energy” data channels every sector, or 32 times per spin. The rate scaler table #2 is shown in Figure 73. These “zero energy” channels correspond to the low energy H^+, He^+, and O^+.

The data used in SPM from the CAMMICE/MICS instrument includes H^+, He^+, and O^+ ions with 24 energy channels from 1 keV to 164 keV. The pitch angle coverage is built up over aggregating the data in 10° pitch angle bins over 5 minutes. The *L* range is built up between *L*=2 and *L*=10 by the Polar orbit sweeping through those ranges of *L*, and in magnetic local time (MLT) by the orbits precession throughout the year. We use data when the MICS instrument is using the Rate Scaler Table 2, from 7 March 1997 until 30 September 1999.

We use two independent versions of the CAMMICE/MICS data set. The first is a set of aggregated files produced by J. Roeder at Aerospace which provide fluxes (cm^{-2} sr^{-1} s^{-1} keV^{-1}) as a function of local pitch angle and energy every 5 minutes, and is referred to as the

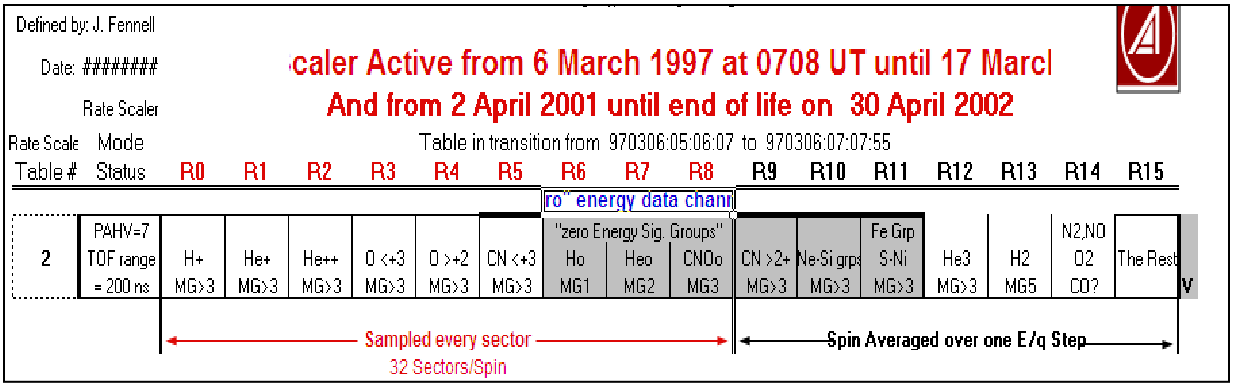

Figure 73. Excerpt from the CAMMICE/MICS rate scaler table #2, showing which measurements get made every sector, corresponding to pitch angle coverage.

"CMICSDB". These are binary files and were produced with efficiency factors determined by J. Roeder in ~2006 (personal communication) to obtain a consistent set of calibrations over the mission duration when doing the analysis for *Roeder et al.* [2005]. The second independent version of the CAMMICE/MICS data was processed by J. Niehof, described in *Niehof* [2011], and is available at http://spacedata.bu.edu/mics.html. The Niehof CAMMICE/MICS data uses the efficiency factors determined circa 1997 and documented by *Niehof* [2011]. This difference of efficiencies makes a marginal difference in the resulting fluxes, and in the absence of a clearly superior data product we use both in AE9/AP9/SPM to provide some measure of uncertainty in the plasma environment.

3.4.1.3 Data processing

This section briefly describes the procedures to go from the CAMMICE/MICS data files identified in Section 3.4.1.2 to the data aggregated into the SPM model. This section includes energy binning, building "composite channels" for each species that span the energy range of the model, and determining magnetic ephemeris. The details of these procedures will be documented elsewhere.

3.4.1.3.1 Energy binning

The CAMMICE/MICS ESA was capable of stepping through 32 energy per charge channels (1 keV to 417.3 keV). Due to the high voltage power supply being unable to hold the analyzer plates at the highest potentials, only the bottom 24 channels were used (1 keV to 173.3 keV). Also, to increase the statistics at each energy, we averaged every pair of energy channels together, yielding the 12 energy ranges shown in Table 27. This is the same procedure used by *Roeder et al.* [2005].

3.4.1.3.2 Composite channels

Due to the nature of the instrument and various measurement techniques used, not all rate scalers measure all species across the entire energy range. We combine low energy channels with high energy channels to provide "composite" channels whose energy spans the complete range. Before combining them into composite channels, some energies of some channels contain zeros or poor quality measurements because the processing algorithm enforced a total energy measurement before assigning the event to a rate scaler. The "zero energy groups" highlighted in rate scalers R6, R7, and R8 of Figure 74, omits the requirement that each particle leaves a measurement in the solid state detector (total energy measurement). These rate scalers are thus lower energy measurements of each species, and can be combined with the higher energy channels to span the range. The logic we use to combine the high energy channels (R0: H^+, R1: He^+, R3: O^+) with the zero energy channels (R6: H, R7: He, R8: O) into H^+, He^+, and O^+ channels for use in SPM is summarized as:

$$H^+ = H^+(R0) + H\ (R4\ only\ below\ 63.75\ keV)$$

$$He^+ = He^+(R1) + He\ (R5\ only\ below\ 36\ keV)$$

$$O^+ = O^+(R3) + O\ (R6\ only\ below\ 85\ keV)$$

This addition is actually a mask, where the data from the "zero energy" rates over-writes the data from the energy-resolved rates, if it exists. Graphically this combination of 6 channels to form complete energy coverage of 3 species is shown of Figure 74.

Table 27. CAMMICE/MICS channel energies.

Channel	Center Energy (keV)
1	1.15
2	2.1
3	3.7
4	6.5
5	11.55
6	20.4
7	36.0
8	63.75
9	85.0
10	105.9
11	131.9
12	164.3

3.4.1.3.3 Magnetic ephemeris calculation

The Polar ephemeris used to compute the magnetic coordinates of the SPM plasma model were obtained from CDAWeb (http://cdaweb.gsfc.nasa.gov/), and were the "predicted" ephemeris. The "predicted" ephemeris is the recommended version [Roeder, Niehof, private communication 2011]. We use this ephemeris to determine the local and minimum magnetic field value at this location in the Olson-Pfitzer-Quiet (OPQ) magnetic field model, the McIlwain formulation (L_m) of the L-value, and the magnetic local time (MLT). We also determine the equatorial pitch angle according to

$$\propto_{eq} = \mathrm{asin}(\sin(\propto_{local})\sqrt{\frac{B_{min}}{B_{local}}}) \tag{83}$$

using B_{min}, B_{local}, and the local pitch angles. We use the IRBEM library to compute these magnetic coordinates (irbem.sf.net).

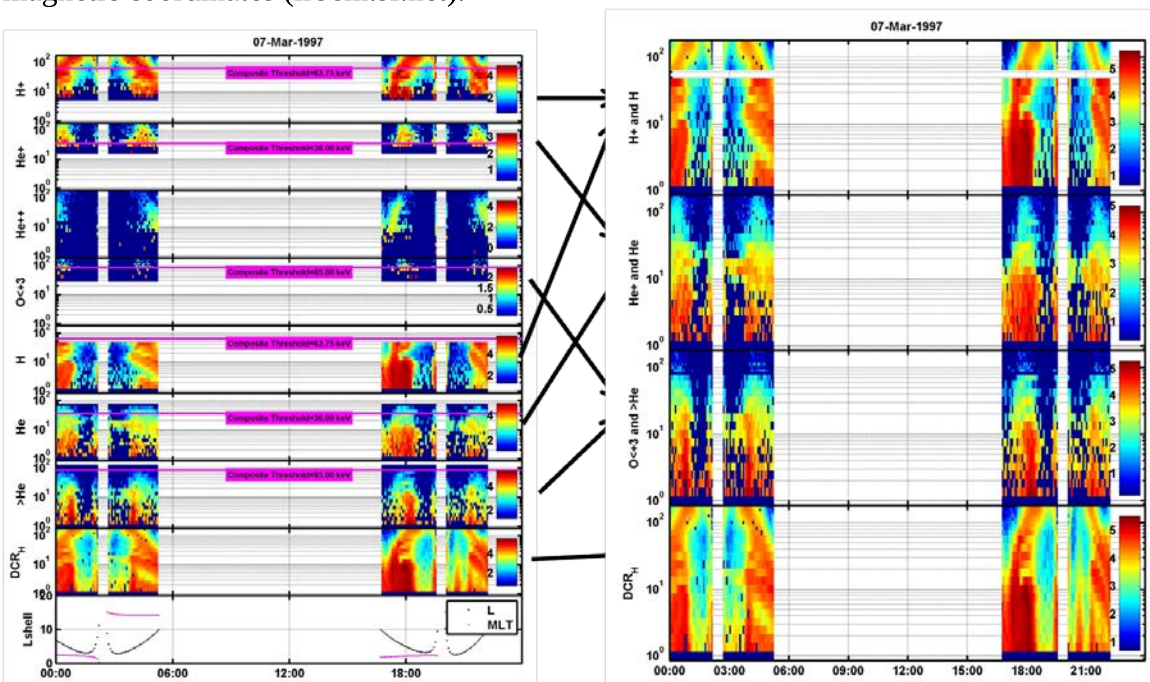

Figure 74. Composite channels from individual rate scalers for March 7, 1997.

3.4.1.3.4 Data set verification in aggregate

To verify we have obtained a clean, appropriate data set to ingest into the SPM framework we compare the data set we have obtained with prior published aggregations of the space plasma environment from these and other measurements. We have done this aggregation and inspection in lieu of a formal "data cleaning" process. For the CAMMICE/MICS data sets we aggregate the observations into natural dimension of the space plasma environment *L*, MLT, equatorial pitch angle, energy and species, as *Roeder et al.* [2005] did. By inspecting the results as a function of all of these dimensions and comparing with the *Roeder et al.* [2005] results, we gain confidence that our data set, in aggregate, yields similar results to the generally accepted picture of the space plasma environment produced by instrument Co-Is and the science community (through peer review).

To produce the results below, we perform a simple binning of the H^+, He^+, and O^+ data in the CAMMICE/MICS data sets. The dimensions into which the data set is binned includes the same binning as was used in *Roeder et al.* [2005]; $2 < L < 10$ in steps of 0.5, MLT from 0 to 24 in 2 hour steps, equatorial pitch angles from $0° < \alpha < 90°$ in 10° steps, and 12 energy steps from 1 keV < E < 164 keV, and 3 species (H^+,He^+, O^+). We aggregated the 5-minute timeseries for March 1997 through Sept 1999 into the 5 dimensional database and plot the results in various dimensions below. This procedure is modeled after the examples given by *Milillo et al.* [2001] and *Roeder et al.* [2005], and described more fully in *Guild et al.* [2013].

3.4.1.3.4.1 H+ verification

Here we present slices of the comparison of our aggregation of the Roeder and Niehof CAMMICE/MICS data set with the aggregation of that data set as assembled for the publication of *Roeder et al.* [2005]. Figure 75 shows mean equatorial pitch angle distributions of the CAMMICE/MICS-Roeder data set at one bin in local time (MLT=18-20) and four *L* values for the aggregation of the Roeder files (thick curves) and the *Roeder et al.* [2005] database (thin curves). In each pitch angle distribution there are 5 colored curves plotted corresponding to different energies. Our aggregation only bins pitch angles from 0° to 90°, ignoring any northward or southward asymmetries, which according to the thin lines of *Roeder et al.* [2005] seems to be a good assumption. For all *L* values, the higher energy PADs are steeper, and the aggregation of our files reasonably agree with the Roeder results, except for very low *L* (top left panel, *L*=3.5). This is largely because our database starts with the transition to Rate Scaler Table #2 in March 1997, not launch as the Roeder database did. *Roeder et al.* [2005] assumed a low-energy pitch angle distribution for the early measurements and averaged that into the database [Roeder, private communication 2011]. We chose not to use those times, when Polar was preferentially sampling the very inner magnetospheric plasma below *L*=4.

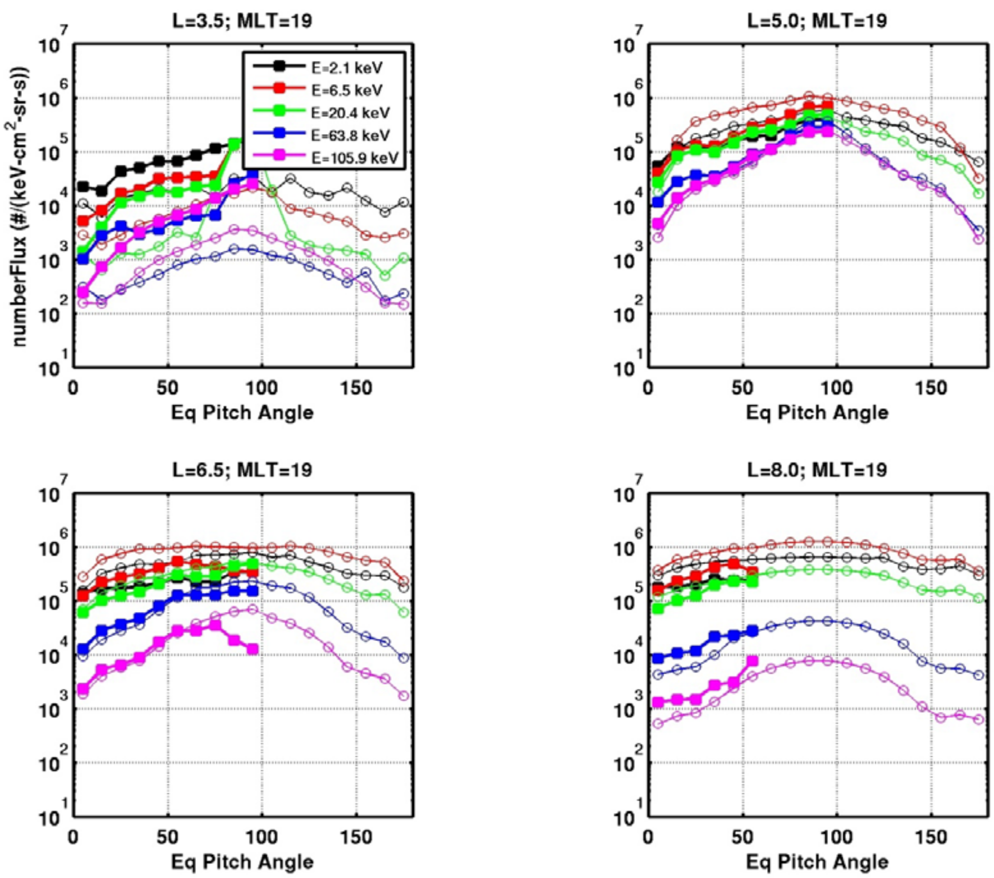

Figure 75. Mean pitch angle distributions aggregated from the Roeder files (thick lines) and Roeder's 2005 database (thin lines).

Another important inspection of the data set is the mean spectra at various *L* values and MLTs, as shown in Figure 76. Now each of the four panels is a spectra of mean H^+ observations at an equatorial pitch angle of 25°, but in four local times around the Earth. Each plot shows 6 colored spectra corresponding to different *L* values from $5 < L < 10$. Thick lines correspond to the aggregation of our CAMMICE/MICS-Roeder data set and thin lines correspond to the Roeder aggregation. The close correspondence of the thin lines with thick lines for each color lends confidence to the data set and our use thereof.

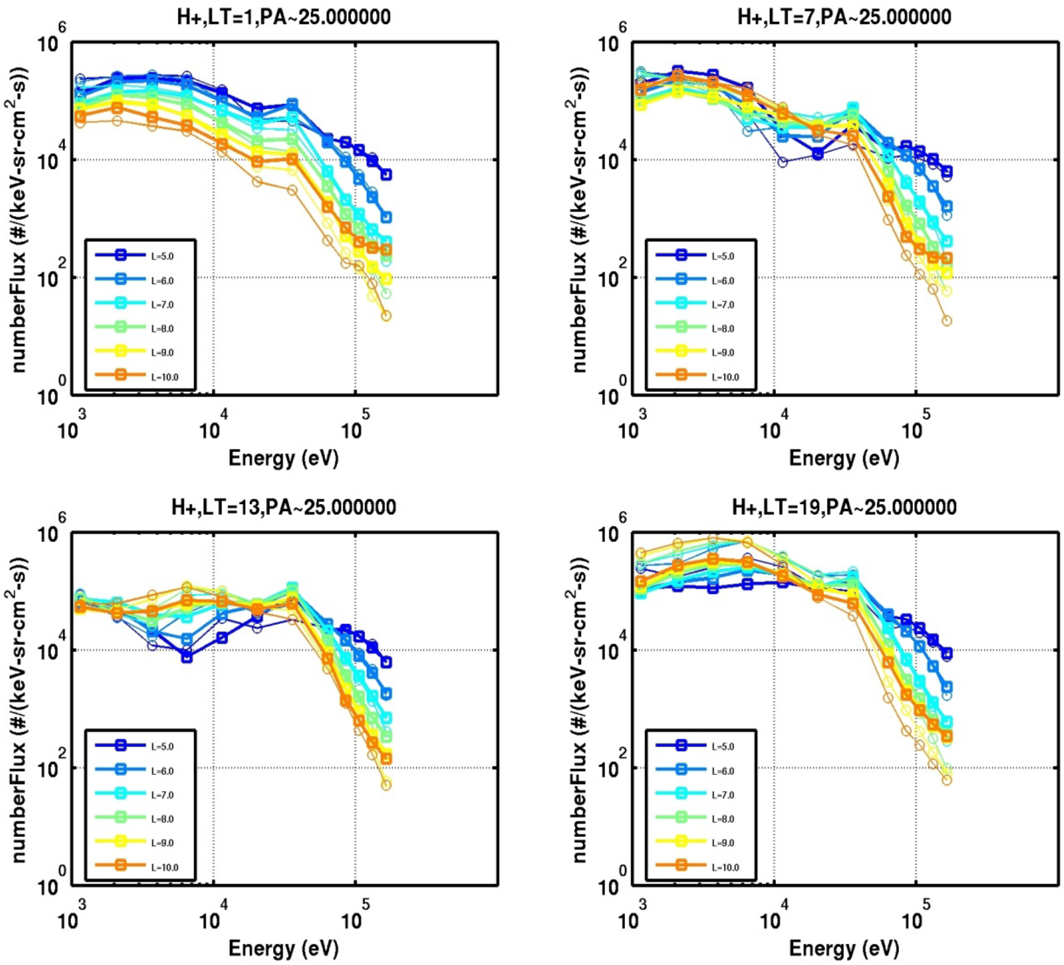

Figure 76. Spectra at an equatorial pitch angle of 25° and four different local times near midnight (top left), dawn (top right), noon (bottom left), and dusk (bottom right). In each panel spectra are colored by *L* value, thin lines are taken from the *Roeder et al.* [2005] database, and thick lines are aggregated in our analysis.

Yet another way to look at the data is with an energy-*L* spectrogram which plots the flux (color) as a function of energy (*y*-axis) and *L* (*x*-axis). An example of this analysis is shown in Figure 77. The figure shows energy-*L* spectrograms for 4 local times (top to bottom) on the left. Features present in these spectrograms are similar as those shown in Milillo et al., using AMPTE/CCE/CHEM data and in *Wang et al.* [2011], using GEOTAIL and THEMIS data. The distribution of individual 5-minute energy-angle measurements included in this MLT bin is shown as the inset histogram of each spectrogram.

The right panel of Figure 77 shows the mean flux ratio between the results in the left panel and the *Roeder et al.* [2005] database. The color scale is logarithmic and goes from a factor of 100 overestimate (red) to a factor of 100 underestimate (blue) of *Roeder et al.* [2005] results. Throughout most of the energy-*L* space, the ratio is largely near 1 (white), with the exception of the low-*L* region. As mentioned above, this is due to the omission of early CAMMICE data when MICS was in mode 1.

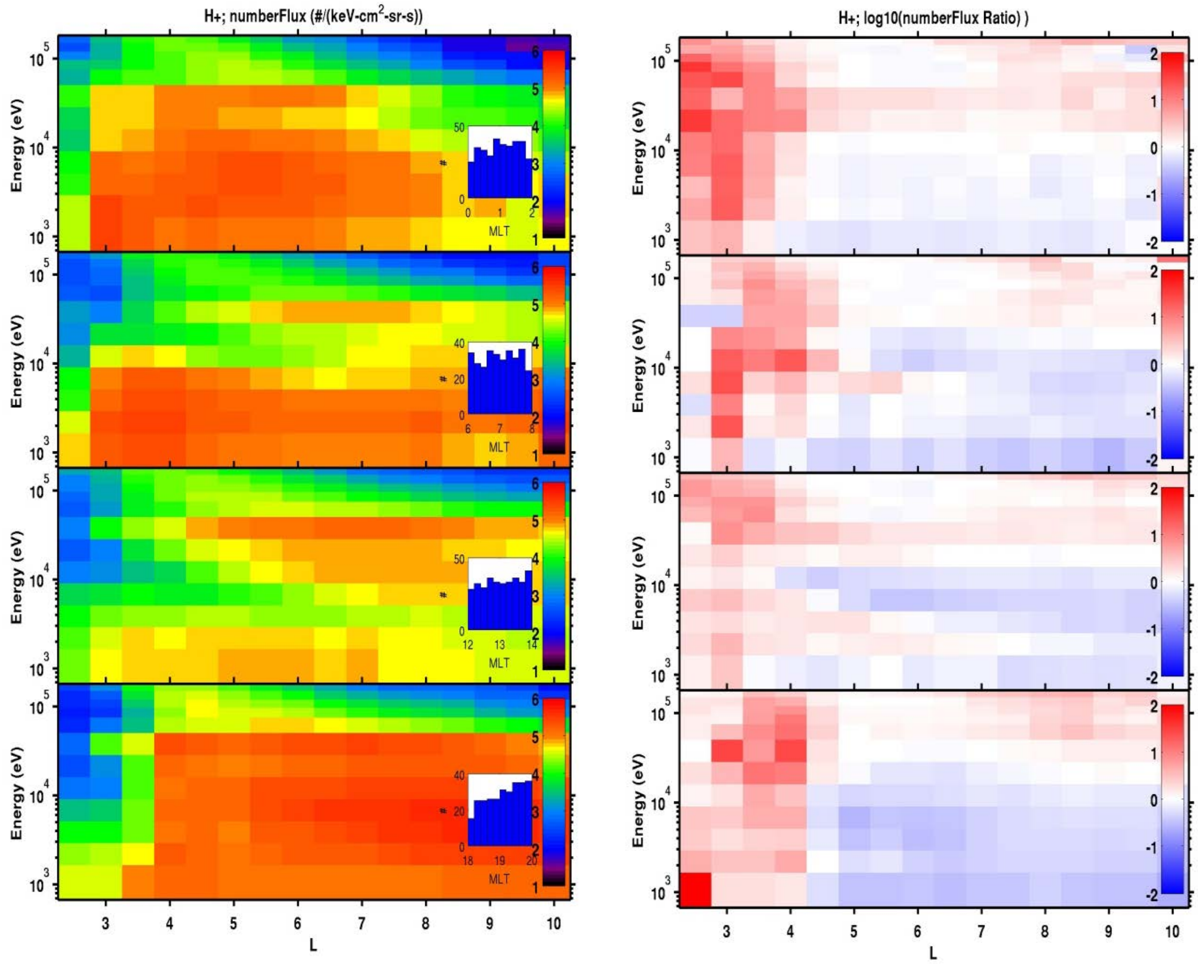

Figure 77. Energy-L spectrograms at four different local times (left) and their flux ratios with the *Roeder et al.* [2005] database (right).

Finally, equatorial flux maps of H^+ are shown in the top panel of Figure 78. The top row shows maps in the XY (GSM) equatorial plane, colored in $\log_{10}$(flux) as the earlier plots. The sun is to the left. Maps range in energy from 1 keV at left to 85 keV at right, and illustrate the local time asymmetries inherent in the plasma environment. *This local time structure is averaged over in the AE9/AP9/SPM model*. The bottom panel of Figure 78 again takes the ratio of the maps in the top panel to the fluxes in the *Roeder et al.* [2005] database. The colors now range from 0.01 to 100 in logarithmic steps, and slightly underestimate the *Roeder et al.* [2005] fluxes for low energies and (light blue in the left panel) and overestimate the *Roeder et al.* [2005] fluxes inside *L*=4 (red near the center of the map). We underestimate Roeder slightly because unlike their database we're including zeros in the averaging, and we overestimate fluxes in the inner magnetosphere because they used more data from Rate Scaler Table 1, when POLAR sampled $L<4$, albeit with a fitted pitch angle distribution.

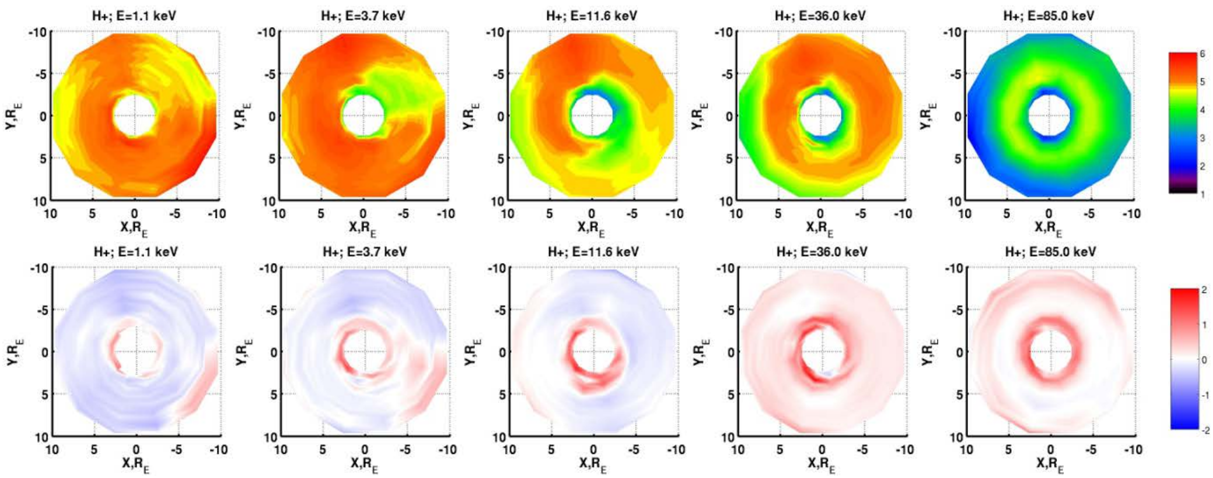

Figure 78. Equatorial flux maps of H^+ (top) along with ratios of these maps with *Roeder et al.* [2005] maps (bottom).

3.4.1.3.4.2 Verification of Niehof data, He^+ and O^+

Figures of this format for the CAMMICE/MICS-Niehof H^+ data set are similar to the results presented above and are shown in Appendix K. Results for He^+ and O^+ are also presented in Appendix K.

3.4.1.3.5 Filtering

This process of verification highlighted some problems inherent with the CAMMICE/MICS data set, forcing us to filter out certain portions of it. For instance, the Roeder datafiles have three intervals of anomalously high fluxes near noon which pulls up the average in that bin. The fluxes are high only in the 10-12 local time bin, as shown in the spectra shown in Figure 79. The fluxes in the original time series files which contribute to these large averages are only a few anomalous intervals when the instrument was not operating properly (21 May 1998 at ~2200 UT, 06 March 1999 at ~1600 UT, and 21 May 1999 at ~1800 UT). There were so few points affected that the feature did not manifest in the turnkey system, which determines the statistics of the median and 95th percentile (or 95th percentile minus the median). We therefore recorded the affected times but the software filtered them out in the routine generation of the runtime tables.

3.4.1.4 Summary

The CAMMICE/MICS instrument contributed H^+, He^+, and O^+ measurements used in AE9/AP9/SPM. We used two independent versions of the data set, one from *Roeder et al.* [2005] and one from *Niehof* [2011]. They largely agree with each other. We cross-calibrated these data sets with LANL/MPA while in magnetic conjunction, and determine cross-calibration factors and residual uncertainties. By binning the data sets and comparing with results of *Roeder* *et al.* [2005], we gain confidence that these data sets, in aggregate, are both used correctly in SPM and representative of the inner magnetospheric plasma population.

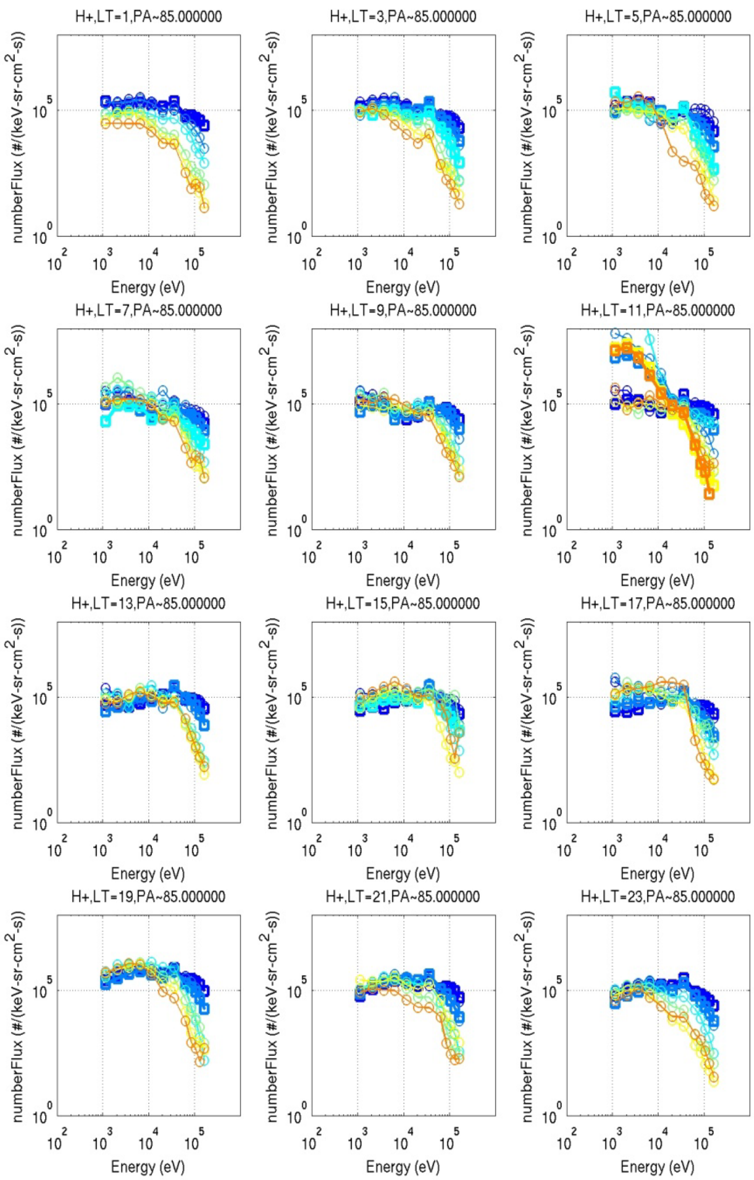

Figure 79. Spectra of the aggregated Roeder files at an equatorial pitch angle of 85° and every 2-hour bin of local time. Anomalous fluxes at low energy show up in the 1100 local time bin, highlighted in the second row, third column by a red arrow.